Analysis of the recombination mechanisms of a silicon solar cell with low bandgap-voltage offset

André Augusto,[a] Stanislau Y. Herasimenka, Richard R. King, Stuart G. Bowden, and Christiana Honsberg
Arizona State University, Electrical Engineering, P.O. Box 875706 Tempe, Arizona 85287-5706, USA

(Received 26 January 2017; accepted 11 May 2017; published online 31 May 2017)

The mathematical dependence of bandgap-voltage offset on Auger and radiative recombination is derived. To study the recombination near the intrinsic limit, we manufacture thin silicon heterojunction test structures designed to minimize surface recombination, and to measure voltages and effective lifetimes near the Auger and radiative limit. Open-circuit voltages over 760 mV were measured on 50-μm-thick structures, leading to bandgap-voltage offsets at open-circuit down to 0.35 V. The Auger and radiative recombination represents over 90% of the recombination at open-circuit. This dominance also holds at the maximum power point, giving pseudo-fill factors of 86%. We demonstrate the potential of thin silicon devices to reach high voltages, and bandgap-voltage offsets in line with the best reported for direct bandgap materials such as gallium indium phosphide and gallium arsenide. *Published by AIP Publishing.*
[http://dx.doi.org/10.1063/1.4984071]

I. INTRODUCTION

Indirect bandgap materials such as crystalline silicon, germanium, and gallium-phosphide, which are limited by Auger recombination rather than radiative recombination, have a lower detailed balance efficiency limit than radiative materials,[1] due to a lower open-circuit voltage, V_{OC}. The open-circuit voltage varies greatly across different materials due to the wide range of energy bandgaps. For experimental solar cells, a measure of the quality of the device is the bandgap-voltage offset at open-circuit, Equation (1), W_{OC}[2]—the lower the value of W_{OC}, the lower the recombination and the better the device. The bandgap-voltage offset at open-circuit is defined as

$$W_{OC} = \frac{E_g}{q} - V_{OC}, \tag{1}$$

where E_g is the energy bandgap and q is the elementary charge. Since at the same excitation (light) level, the energy difference between the electron and hole quasi-Fermi levels and their respective band edges is remarkably similar in different semiconductors, much of the change in V_{OC} is due to the change in bandgap E_g, and W_{OC} varies over a much smaller range than E_g, allowing easier comparison across different materials.

The W_{OC} measured on high efficiency direct bandgap materials typically shows values below 0.4 V.[2] The best W_{OC} reported at one sun (0.100 W/cm^2) was measured on a thin gallium arsenide (GaAs) solar cell with a rear reflector for photon recycling. The W_{OC} was 0.298 V, assuming a bandgap of 1.42 eV.[3,4]

Just recently, silicon solar cells surpass the 720 mV open-circuit voltage, and consequently the 0.4 V barrier. Open-circuit voltages of 750 mV were reported on silicon heterojunction solar cells (SHJ),[5] corresponding to a W_{OC} approximately of 0.370 mV, assuming E_g equal to 1.121 eV at 25 °C and no bandgap narrowing. Equation (1) shows that higher voltages are a requisite to improve W_{OC}. Higher voltages require high quality surface passivation,[6] and thinner wafers, as the V_{OC} increases as a function of the excess carrier density.[7,8] The SHJ solar cell architecture[9] provides remarkable passivation of the surfaces.[10] High quality passivation is accomplished by using hydrogenated amorphous silicon[11] as the high-bandgap barrier layer separating the absorber from highly recombination-active (ohmic) contacts.[12]

In this work, we derive the dependence of bandgap-voltage offset on Auger and radiative recombination. To study the recombination near the intrinsic limit, we manufacture thin silicon heterojunction test structures designed to minimize surface recombination, and to measure voltages and effective lifetimes near the Auger and radiative limit. The reasons for high open-circuit voltages and low W_{OC} are discussed using recombination component modeling, showing an effective minority-carrier lifetime within a factor of 10% of the Auger lifetime limit at open-circuit, enabling high V_{OC}'s, FF's, and small W_{OC} values. These results also show that Auger and radiative recombination represents over 90% of the recombination that is limiting the V_{OC} and W_{OC}. With this study, we show the potential of thin silicon solar cells to reach high voltages, and W_{OC} comparable to the best gallium indium phosphide (GaInP) solar cell.[13]

II. INTRINSIC BANDGAP-VOLTAGE OFFSET

The bandgap-voltage offset can be expressed in terms of the recombination of electron-hole pairs, similar to the open-circuit voltage. The total recombination in a sample of thickness w can be expressed as a function of excess minority-carrier density, Δp (for n-type material), and effective minority-carrier lifetime,[14] τ_{eff}

[a]Author to whom correspondence should be addressed: augusto@asu.edu

$$J_{rec} = \frac{q\,w\,\Delta p}{\tau_{eff}}, \tag{2}$$

where J_{rec} is recombination current density. In a solar cell operating under open-circuit conditions and steady-state illumination, the photogeneration current density, J_{ph}, and the recombination current density of electron-hole pairs are balanced, $J_{ph} = J_{rec}$. The photogenerated excess electron and hole densities are balanced too, $\Delta p = \Delta n$. The voltage can be written as a function of electron, n, and hole, p, concentrations

$$V = \frac{k\,T}{q}\ln\left(\frac{n\,p}{n_i^2}\right), \tag{3}$$

where the intrinsic carrier concentration, n_i, is a strong function of bandgap, and also of the densities of states in the valence band, N_V and conduction band, N_C

$$n_i^2 = N_V N_C e^{-\frac{E_g}{kT}}, \tag{4}$$

where k is the Boltzmann constant and T is the temperature. To remove this strong E_g dependence, one can write[2]

$$W \equiv \frac{E_g}{q} - V = \frac{kT}{q}\ln\left(\frac{N_V N_C}{n_i^2}\right) - \frac{kT}{q}\ln\left(\frac{np}{n_i^2}\right) = \frac{kT}{q}\ln\left(\frac{N_V N_C}{np}\right), \tag{5}$$

where $W \equiv (E_g/q) - V$ is the bandgap-voltage offset under general bias conditions.

At high level injection $n = p = \Delta p$, and the intrinsic carrier concentration needs to be corrected to include the bandgap narrowing,[15] ΔE_g. Using Equations (2) and (3), the open-circuit voltage can be expressed as

$$V_{OC} = \frac{k\,T}{q}\ln\left(\frac{J_{ph}\,\tau_{eff}\,\Delta p}{q\,w\,n_{i,eff}^2}\right), \tag{6}$$

where the effective intrinsic carrier concentration, $n_{i,eff}$, is given by

$$n_{i,eff}^2 = n_i^2 e^{\frac{\Delta E_g}{kT}}. \tag{7}$$

Finding W_{OC} with respect to the narrowed bandgap $E_g = E_{g0} - \Delta E_g$ at the injection level corresponding to Δp, the main dependence of W_{OC} on the bandgap can be separated out using Equations (4) and (6)

$$W_{OC} = \frac{E_{g0} - \Delta E_g}{q} - V_{OC} = \frac{k\,T}{q}\ln\left(\frac{q\,w\,N_V\,N_C}{J_{ph}\,\tau_{eff}\,\Delta p}\right), \tag{8}$$

where E_{g0} is the bandgap without bandgap narrowing (e.g., 1.121 eV for crystalline silicon at 25 °C). The τ_{eff}, N_C and N_V depend somewhat on E_g, and w and J_{ph} depend on device design, but the main point is that since these parameters appear in the logarithm, W_{OC} depends only weakly on the bandgap, resulting in a nearly constant bandgap-offset voltage across different materials. W_{OC} has been calculated as a function of radiative recombination,[2] since this is the fundamental limiting recombination mechanism for direct bandgap materials. Crystalline silicon, an indirect bandgap material, is limited by Auger recombination. The Auger lifetimes, τ_{Auger}, can be approximated for high-injection level conditions as[16]

$$\tau_{Auger} = \frac{1}{C\,\Delta p^2}, \tag{9}$$

where C is the ambipolar Auger recombination coefficient, which for crystalline silicon was found to be 1.66×10^{-30} $cm^6\,s^{-1}$ in the range of $10^{15} < \Delta p < 2 \times 10^{17}\,cm^{-3}$,[17] this is the range of the V_{OC} injection level for crystalline silicon solar cells. Using Equations (2) and (8)

$$\Delta p = \left(\frac{J_{ph}}{q\,w\,C}\right)^{\frac{1}{3}} \tag{10}$$

at open-circuit. From Equation (3) at high injection level such that $n = p = \Delta p$, n_i is replaced by $n_{i,eff}$, resulting in

$$V_{OC,\,Auger} = \frac{k\,T}{q}\ln\left(\frac{1}{n_{i,eff}^2}\left(\frac{J_{ph}}{q\,w\,C}\right)^{\frac{2}{3}}\right) \tag{11}$$

and from Equation (5)

$$W_{OC,\,Auger} = \frac{k\,T}{q}\ln\left(N_V\,N_C\left(\frac{q\,w\,C}{J_{ph}}\right)^{\frac{2}{3}}\right), \tag{12}$$

where $W_{OC,Auger}$ is the bandgap-voltage offset at open circuit limited by Auger recombination. When the intrinsic lifetime, τ_{int}, in high level injection is limited by the Auger and radiative lifetimes

$$\frac{1}{\tau_{int}} = \frac{1}{\tau_{Auger}} + \frac{1}{\tau_{rad}} = C\,\Delta p^2 + B\,\Delta p \tag{13}$$

where B is the radiative recombination coefficient. Thus at open-circuit

$$J_{ph} = J_{rec} = \frac{q\,w\,\Delta p}{\tau_{eff}} = q\,w\,\Delta p\left(C\,\Delta p^2 + B\,\Delta p\right) \tag{14}$$

so that

$$\Delta p = \left(\frac{J_{ph}}{q\,w\,(C\,\Delta p + B)}\right)^{\frac{1}{2}} \tag{15}$$

and from Equation (5)

$$W_{OC,\,int} = \frac{k\,T}{q}\ln\left(\frac{N_V\,N_C\,q\,w\,(C\Delta p + B)}{J_{ph}}\right), \tag{16}$$

where $W_{OC,int}$ is the bandgap-voltage offset at open-circuit limited by intrinsic recombination, i.e., Auger and radiative recombination.

III. EXPERIMENTAL DETAILS

The SHJ test structures were prepared on commercial grade n-type Czochralski wafers with 3.5–4 Ω cm resistivity, ⟨100⟩ orientation, and initial thickness of 145 μm. The

wafers were thinned down to 50 μm via alkaline wet etching, followed by wet chemical cleaning. The wafers were not textured. The SHJ was formed using plasma enhanced chemical vapor deposition (PECVD) to grow 15 nm intrinsic a-Si:H (i) and 7–10 nm doped a-Si:H (p+, n+) on both sides of the c-Si wafer, forming a p/i/n/i/n stack. The intrinsic layer was grown in three steps: first a thinner intrinsic layer (5 nm) was grown, followed by hydrogen plasma treatment (HPT), and finally a thicker layer of 10 nm was grown on top. The increase of lifetime when HPT is applied is due to diffusion of hydrogen atoms to the a-Si:H(i)/c-Si-interface[18] and improved chemical passivation due to dangling bond saturation, reducing the density of defects at the surface of silicon.[19] A thinner intrinsic layer was first grown to promote a proper diffusion of the hydrogen to the a-Si:H(i)/c-Si-interface shown in Figure 1. The samples were finished by sputtering 80 nm of indium tin oxide (ITO) on the front side and 280 nm on the rear side. The rear ITO has low absorption in the infrared region.[20] Two different sputtering RF powers were tried, to see the effect in the surface passivation. The samples were then annealed at 200 °C for 30 min.

The V_{OC} was measured at a fixed temperature of 25 °C with a spectrum to match the standard terrestrial spectrum of AM1.5. The light intensity varies from 0.05 to 2 suns where a sun is defined as 100 mW/cm^2. Plotting one minus suns (1-suns) vs the V_{OC} gives a Suns-V_{OC} curve. Scaling the Suns-V_{OC} curve with the short-circuit current converts the Suns-V_{OC} to a curve like the light IV curve but without the effect of series resistance. Since the fill-factor is a ratio, a fill-factor can be determined from the Suns-V_{OC} curve directly and is termed the pseudo-fill factor (pFF).[21] A further advantage of the Suns-V_{OC} is that it relies on a voltage measurement of the cell so it can also be done directly on the ITO without the need for metal contacts.[22]

Effective minority-carrier lifetime was measured before and after ITO sputtering using a Sinton lifetime tester using photoconductance.[14] Instead of interpreting the carrier concentration from the photoconductance as a measure of lifetime, it can equally be interpreted as a measure of the cell implied open-circuit-voltage using Equation (3). Similar to the Suns-V_{OC} measurements described above the implied-V_{OC} is also measured as a function of light intensity and then plotted as implied-V_{OC} vs (1-suns). A fill factor of the curve is then calculated to give the implied-FF (iFF). The implied V_{OC} at one sun light intensity is denoted as iV_{OC}.

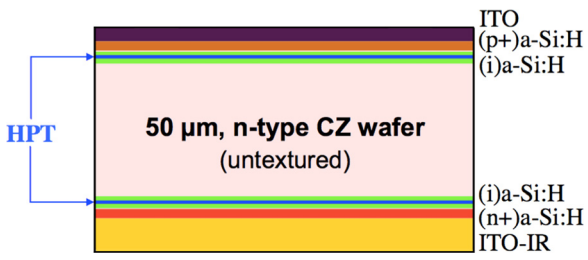

FIG. 1. SHJ test structure. The wafer was not textured to minimize the surface recombination. The (i)a-Si:H is performed in two steps, and HTP is applied between those steps.

IV. RESULTS AND DISCUSSION

Figure 2 shows the measured effective minority-carrier lifetime as a function of excess carrier density before and after ITO sputtering. The samples with a RF sputtering power of 3 kW show a considerable degradation of the lifetime after ITO sputtering. Even after annealing treatment,[23] the lifetime is nearly half of that before sputtering. On the other hand, the samples sputtered with lower RF power show little effective minority-carrier lifetime degradation after sputtering. Lower power ITO sputtering reduced defect formation in the a-Si layers and at the a-Si/c-Si interface leading to substantial improvement of effective minority-carrier lifetime, especially near the maximum power injection levels. As a result, the implied-fill factor (iFF) of the cells with ITO sputtered at lower power increased from 85% to 86%. The HPT passivated the silicon across the entire minority-carrier injection range. For thin wafers, we see improvements in the effective minority-carrier lifetime of over 1 ms when HPT is used.

To better understand the recombination processes, the effective minority-carrier lifetime was broken down into its component parts

$$\tau_{eff} = \left(\frac{1}{\tau_{Auger}} + \frac{1}{\tau_{SRH}} + \frac{1}{\tau_{rad}} + \frac{1}{\tau_S}\right)^{-1}, \tag{17}$$

where each part corresponds to a recombination mechanism. τ_{Auger}, τ_{rad}, and τ_{SRH} are due to bulk Auger, radiative, and Shockley-Read-Hall (SRH) recombination, respectively, and τ_S is due to the recombination at the front and rear surfaces. The Auger and radiative recombination were calculated using Richter parametrization, see the Appendix,[16] which includes the Schenk bandgap narrowing model[15] and injection dependent radiative recombination.[24] SRH bulk recombination was measured on companion 200 μm wafers and is labeled SRH in Figure 3. In our thin samples, the front

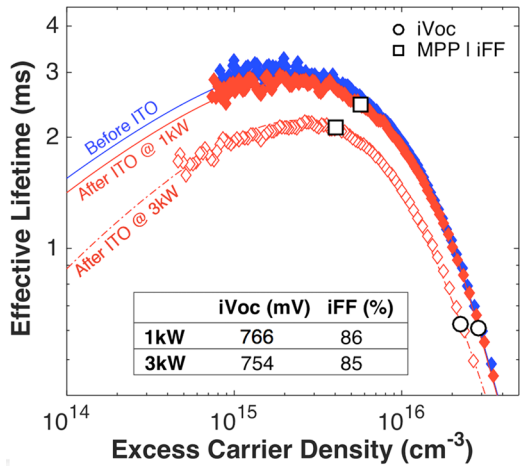

FIG. 2. Effective minority-carrier lifetime vs. excess carrier density measured on a representative wafer after ip/in deposition and after ITO deposition. Similar lifetimes are obtained on both samples before ITO deposition. However, significant degradation of the effective minority-carrier lifetime is observed after sputtering at a RF power of 3 kW, even after annealing at 200 °C for 30 min. The iV_{OC} and iFF values are from the effective minority-carrier lifetime measurements using the Sinton lifetime tester.

surface is in inversion and the rear in accumulation due to the doped layers. Under these conditions, the surface behaves like an emitter region[25] and the surface recombination current density J_S can be written within the double-diode model[26]

$$J_S = qWR_S = 2J_{01}\left(e^{\frac{qV}{n_{01}KT}} - 1\right) + J_{02}\left(e^{\frac{qV}{n_{02}KT}} - 1\right), \quad (18)$$

where J_{01} and J_{02} determine the recombination current densities associated with n_{01} and n_{02}. In its simplest interpretation, J_{01} with n_{01} around 1 is assigned to the surface passivation quality and contains a factor of two since it results from both front and back surfaces. The J_{02} with n_{02} around 2 is assigned to recombination in the space-charge region[27] for the front in inversion region. The J_{01} is determined from effective minority-carrier lifetime measurement at a high injection level,[28] where J_{02} is negligible. Using the recombination rate, R_s, and the effective surface lifetime, τ_s, the effective surface recombination velocity, S, is calculated for a given cell thickness, w, and excess carrier density, Δp

$$\tau_S = \frac{\Delta p}{R_S}, \quad (19)$$

$$S = \frac{w}{2.\tau_S}. \quad (20)$$

For 50 μm thickness and excess carrier density of 1×10^{15} cm^{-3}, the surface recombination velocity of the sample sputtered at 1 kW is very low at 0.6 cm s^{-1}, and is 1.2 cm s^{-1} for the one sputtered at 3 kW. Figure 3 shows the components of the effective minority-carrier lifetime as a function of the injection levels after ITO sputtering. For solar cells with measured surface saturation current density (J_{01}) equal to 0.1 fA cm^{-2} and measured J_{ph} of 38.8 mA cm^{-2}, the model indicates that Auger recombination is responsible for over 82% of the recombination at V_{OC} (compared to 70% in the samples sputtered at 3 kW), while the contribution of bulk SRH is around 7%, bulk radiative is 9%, and the remaining 2% corresponds to surface recombination mechanisms.

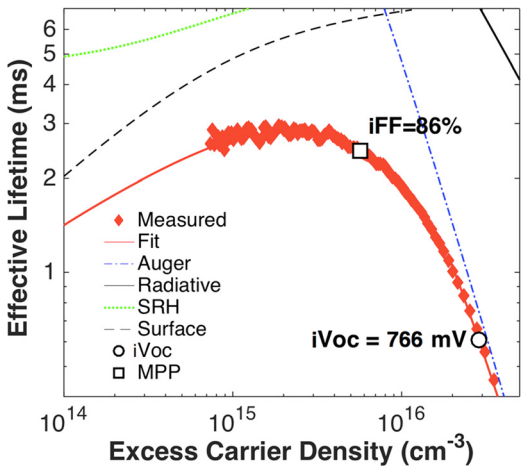

FIG. 3. The components of the effective minority-carrier lifetime due to different recombination mechanisms after ITO sputtering.

TABLE I. The iV_{OC} and iFF result from the effective minority-carrier lifetime measurements, and the V_{OC} and pFF are measured using the Suns-V_{OC} tester. The temperature control (set to 25 °C) on Suns-Voc and lifetime tester can have temperature fluctuations of ±1 °C leading to variations of ±2 mV. W_{OC} is calculated using Equation (8) with $Eg_0 = 1.121$ eV and ΔEg equal to 6.5 mV for the samples sputtered at 1 kW and 6.1 mV for the samples sputtered at 3 kW.

Power kW	iV_{oc} mV	iFF %	V_{oc} mV	pFF %	W_{oc} mV
3	754	85	753	84	360
1	766	86	764	85	349

The V_{OC} and pFF were measured in the Suns-V_{OC}. The values were measured using a probe station and they are local values. Due to inhomogeneity in the sputtering deposition of ITO, the V_{OC} varies slightly across the wafer with an average value of 761 mV and individual values ranging from 759 to 764 mV. These open-circuit voltages lead to W_{OC} values down to 0.350 V, see Table I. W_{OC} is calculated using Equation (8).

For sufficiently low surface recombination [≤5 cm/s (Refs. 29)], a thinner wafer results in a higher excess carrier density and an increase of the V_{OC}. Considering the Auger and radiative recombination mechanisms as well as the Lambertian light trapping limit,[30] the intrinsic V_{OC} and W_{OC} are shown in Figure 4 as a function of the wafer thickness assuming wafers with 4 Ω.cm resistivity. The intrinsic W_{OC} is calculated using Equation (16). For a 50 μm-thick solar cell, the V_{OC} intrinsic limit is 769 mV. If we replace the maximum J_{ph} given by the Lambertian limit by our measured J_{ph} of 38.8 mA cm^{-2} the V_{OC} limit would be 767 mV, very close to our measured V_{OC} of 764 mV. In Figure 4, we also show recent experimental results of high V_{OC} for silicon solar cells[5,6] and the corresponding W_{OC}, including the world record silicon solar cell.[31] The W_{OC} values were calculated from measured V_{OC} using Equation (1).

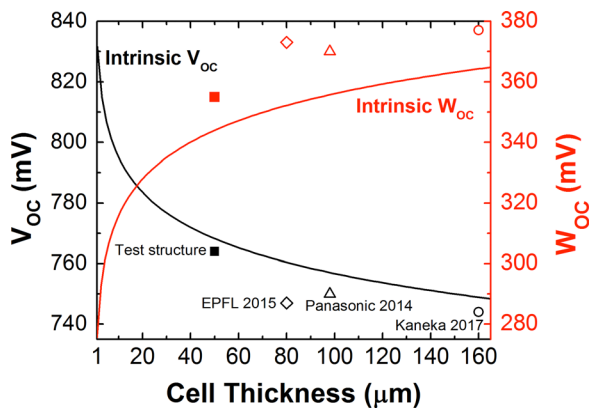

FIG. 4. Intrinsic open-circuit voltage (black curve) and intrinsic bandgap offset open-circuit voltage (red curve) as a function of cell thickness, considering the Auger, the radiative recombination mechanisms as well as the Lambertian light-trapping limit. Recent experimental results of high V_{OC} for silicon and the corresponding W_{OC} are shown for Refs. 5, 6, and 31. The W_{OC} values were calculated from measured V_{OC} using Equation (1) with E_g equal to 1.121 eV.

V. CONCLUSIONS

The bandgap-offset at open circuit voltage depends weakly on the bandgap, resulting in a nearly constant bandgap-offset voltage across different materials. Thus, there is a suitable metric to compare the quality of experimental devices regardless of their voltage or bandgap. This work experimentally demonstrates bandgap-voltage offsets in crystalline silicon devices, comparable with the best reported for direct bandgap materials such as GaAs and GaInP, which have higher bandgaps and voltages. By utilizing 50 μm-thick Czochralski silicon wafers, high quality a-Si passivation, and low surface damage sputtering processes it was possible to preserve the initial high minority-carrier lifetime and surpass the hurdle of a 760 mV open-circuit voltage. The surface recombination current density after ITO sputtering is 0.1 fA/cm^2, as a result of extremely good surface passivation improved by the hydrogen plasma treatment, and the use of low power sputtering. Auger recombination is responsible for over 80% of the recombination losses. The dominance of Auger recombination also holds at maximum power point, giving pseudo-fill factors of 86%. Due to inhomogeneity in the sputtering deposition of ITO, the V_{OC} varies slightly across the wafer with an average value of 761 mV and individual values from 759 to 764 mV. The actual V_{OC} nearly matches the implied-V_{OC} indicating the extremely high quality device. The measured V_{OC} is close to the limit imposed by Auger/radiative recombination. The small difference is partly due to the lack of light trapping in our planar test structures. These results are a good indication of the potential of thin crystalline silicon solar cells.

ACKNOWLEDGMENTS

This material was based on work supported in part by the National Science Foundation (NSF) and the Department of Energy (DOE) under NSF CA No. EEC-1041895. We also acknowledge DOD under Grant No. DODRIF13-OEPP01-P-0020.

APPENDIX: AUGER AND RADIATIVE RECOMBINATION

The intrinsic lifetime, τ_{int}, is defined by

$$\frac{1}{\tau_{int}} = \frac{1}{\tau_{Auger}} + \frac{1}{\tau_{rad}}. \tag{A1}$$

The Auger and radiative contributions were estimated using the work of Richter *et al.*[16]

$$\tau_{int} = \frac{\Delta p}{\left(np - n_{i,eff}^2\right)\left(2.5 \times 10^{-31} g_{eeh} n_0 + 8.5 \times 10^{-32} g_{ehh} p_0 + 3.0 \times 10^{-29} \Delta p^{0.92} + B\right)}, \tag{A2}$$

where n_0 and p_0 are the equilibrium electron and hole density, and the enhancement factors are defined by

$$g_{eeh}(n_0) = 1 + 13\left\{1 - \tanh\left[\left(\frac{n_0}{N_{0,eeh}}\right)^{0.66}\right]\right\}, \tag{A3}$$

$$g_{eeh}(p_0) = 1 + 7.5\left\{1 - \tanh\left[\left(\frac{p_0}{N_{0,eeh}}\right)^{0.63}\right]\right\}, \tag{A4}$$

where $N_{0,eeh} = 3.3 \times 10^{17}$ cm^{-3} and $N_{0,ehh} = 7.0 \times 10^{17}$ cm^{-3}. B value is 4.73×10^{-15} cm^3 s^{-1} at 300 K.[32]

[1]W. Shockley and H. J. Queisser, "Detailed balance limit of efficiency of p-n junction solar cells," J. Appl. Phys. **32**, 510–519 (1961).
[2]R. R. King, D. Bhusari, A. Boca, D. Larrabee, X. Q. Liu, W. Hong, C. M. Fetzer, D. C. Law, and N. H. Karam, "Band gap-voltage offset and energy production in next-generation multijunction solar cells," Prog. Photovoltaics **19**(7), 797–812 (2011).
[3]M. A. Green, K. Emery, Y. Hishikawa, W. Warta, and E. D. Dunlop, "Solar cell efficiency tables (version 48)," Prog. Photovoltaics **24**, 905–913 (2016).
[4]B. M. Kayes, H. Nie, R. Twist, S. G. Spruytte, F. Reinhardt, I. C. Kizilyalli, and G. S. Higashi, "27.6% conversion efficiency, a new record for single-junction solar cells under 1 sun illumination," in 37th IEEE Photovoltaic Specialists Conference (2011), pp. 4–8.
[5]K. Masuko, M. Shigematsu, T. Hashiguchi, D. Fujishima, M. Kai, N. Yoshimura, T. Yamaguchi, Y. Ichihashi, T. Mishima, N. Matsubara, and T. Yamanishi, "Achievement of more than 25% conversion efficiency with crystalline silicon heterojunction solar cell," IEEE J. Photovoltaics **4**(6), 1433–1435 (2014).
[6]B. Terheiden, T. Ballmann, R. Horbelt, Y. Schiele, S. Seren, J. Ebser, G. Hahn, V. Mertens, M. B. Koentopp, M. Scherff, J. W. Müller *et al.*, "Manufacturing 100-μm-thick silicon solar cells with efficiencies greater than 20% in a pilot production line," Phys. Status Solidi A **212**(1), 13–24 (2015).
[7]S. Tohoda, D. Fujishima, A. Yano, A. Ogane, K. Matsuyama, Y. Nakamura, N. Tokuoka, H. Kanno, T. Kinoshita, H. Sakata, and M. Taguchi, "Future directions for higher-efficiency HIT solar cells using a thin silicon wafer," J. Non-Cryst. Solids. **358**(17), 2219–2222 (2012).
[8]T. Tiedje, E. Yablonovitch, G. D. Cody, and B. G. Brooks, "Limiting efficiency of silicon solar cells," IEEE Trans. Electron Devices **31**(5), 711–716 (1984).
[9]T. Sawada, N. Terada, S. Tsuge, T. Baba, T. Takahama, K. Wakisaka, S. Tsuda, and S. Nakano, "High-efficiency a-Si/c-Si heterojunction solar cell," in *1st World Conference on Photovoltaic Energy Conversion, Conference Record of the Twenty Fourth IEEE Photovoltaic Specialists Conference* (1994), Vol. 2, pp. 1219–1226.
[10]A. G. Aberle, "Surface passivation of crystalline silicon solar cells: A review," Prog. Photovoltaics **8**, 473–487 (2000).
[11]J. I. Pankove and M. L. Tarng, "Amorphous silicon as a passivant for crystalline silicon," Appl. Phys. Lett. **34**(2), 156–157 (1979).
[12]S. De Wolf, A. Descoeudres, Z. C. Holman, and C. Ballif, "High-efficiency silicon heterojunction solar cells: A review," Green **2**(1), 7–24 (2012).
[13]J. F. Geisz, M. A. Steiner, I. Garcia, S. R. Kurtz, and D. J. Friedman, "Enhanced external radiative efficiency for 20.8% efficient single-junction GaInP solar cells," Appl. Phys. Lett. **103**(4), 041118 (2013).
[14]R. A. Sinton and A. Cuevas, "Contactless determination of current–voltage characteristics and minority-carrier lifetimes in semiconductors from quasi-steady-state photoconductance data," Appl. Phys. Lett. **69**(17), 2510–2512 (1996).

[15]A. Schenk, "Finite-temperature full random-phase approximation model of band gap narrowing for silicon device simulation," J. Appl. Phys. **84**(7), 3684–3685 (1998).
[16]A. Richter, S. W. Glunz, F. Werner, J. Schmidt, and A. Cuevas, "Improved quantitative description of Auger recombination in crystalline silicon," Phys. Rev. B **86**(16), 165202 (2012).
[17]R. A. Sinton and R. M. Swanson, "Recombination in highly injected silicon," IEEE Trans. Electron Devices **34**(6), 1380–1389 (1987).
[18]M. Mews, T. F. Schulze, N. Mingirulli, and L. Korte, "Hydrogen plasma treatments for passivation of amorphous-crystalline silicon-heterojunctions on surfaces promoting epitaxy," Appl. Phys. Lett. **102**(12), 122106 (2013).
[19]A. Cuevas, T. Allen, J. Bullock, Y. Wan, D. Wan, and X. Zhang, "Skin care for healthy silicon solar cells," in 42nd IEEE Photovoltaic Specialist Conference (2015), pp. 1–6.
[20]Z. C. Holman, M. Filipič, A. Descoeudres, D. Wolf, F. Smole, M. Topič, and C. Ballif, "Infrared light management in high-efficiency silicon heterojunction and rear-passivated solar cells," Appl. Phys. Lett. **113**(1), 013107 (2013).
[21]J. Greulich, M. Glatthaar, and S. Rein, "Fill factor analysis of solar cells' current–voltage curves," Prog. Photovoltaics **18**(7), 511–515 (2010).
[22]R. A. Sinton and R. G. Pauley, "Measurement of current-voltage characteristic curves of solar cells and solar modules," U.S. patent US7696461 B2 (13 April 2010).
[23]D. Zhang, A. Tavakoliyaraki, Y. Wu, R. A. C. M. M. Van Swaaij, and M. Zeman, "Influence of ITO deposition and post annealing on HIT solar cell structures," Energy Procedia **8**, 207–213 (2011).
[24]P. P. Altermatt, F. Geelhaar, T. Trupke, X. Dai, A. Neisser, and E. Daub, "Injection dependence of spontaneous radiative recombination in crystalline silicon: Experimental verification and theoretical analysis," Appl. Phys. Lett. **88**(26), 261901 (2006).
[25]S. Olibet, E. Vallat-Sauvain, and C. Ballif, "Model for a-Si: H/c-Si interface recombination based on the amphoteric nature of silicon dangling bonds," Phys. Rev. B **76**(3), 035326 (2007).
[26]M. J. Kerr, "Surface, emitter and bulk recombination in silicon and development of silicon nitride passivated solar cells," Ph.D. thesis (The Australian National University, 2002).
[27]S. Olibet, "Properties interfaces amorphous/crystalline silicon heterojunctions," Ph.D. thesis (Universite de Neuchatel, 2009).
[28]D. E. Kane and R. M. Swanson, "Measurement of the emitter saturation current by a contactless photoconductivity decay method," in 18th IEEE Photovoltaic Specialists Conference (1985), pp. 578–583.
[29]S. Wang and D. Macdonald, "Temperature dependence of Auger recombination in highly injected crystalline silicon," J. Appl. Phys. **112**(11), 113708 (2012).
[30]L. C. Andreani, A. Bozzola, and M. Liscidini, "Light trapping in thin film solar cells: Towards the Lambertian limit," Proc. SPIE **8438**, 84380C (2012).
[31]K. Yoshikawa, H. Kawasaki, W. Yoshida, T. Irie, K. Konishi, K. Nakano, T. Uto, D. Adachi, M. Kanematsu, H. Uzu, and K. Yamamoto, "Silicon heterojunction solar cell with interdigitated back contacts for a photoconversion efficiency over 26%," Nature Energy **2**, 17032 (2017).
[32]T. Trupke, M. A. Green, P. Würfel, P. P. Altermatt, A. Wang, J. Zhao, and R. Corkish, "Temperature dependence of the radiative recombination coefficient of intrinsic crystalline silicon," J. Appl. Phys. **94**(8), 4930 (2003).